49953 52 P.

REPRINTS REMOVED APP A, B & C

January 30, 1987

Annual Report for Grant No. NAGW-319
Covering the Period from 15 May 1986 to 14 January 1987

PHOTOABSORPTION AND PHOTODISSOCIATION OF MOLECULES IMPORTANT IN THE INTERSTELLAR MEDIUM

Submitted by:

Long C. Lee and Masako Suto
Department of Electrical & Computer Engineering
San Diego State University
San Diego, CA 92182

Prepared for:

NASA Headquarters
Washington, D.C. 20546
Attention: Dr. Nancy W. Boggess
Astronomy/Relativity Branch
Code EZ

(NASA-CR-180101) PHOTOABSORPTION AND PHOTODISSOCIATION OF MOLECULES IMPORTANT IN THE INTERSTELLAR MEDIUM Annual Report, 15 May 1986 - 14 Jan. 1987 (San Diego State Univ., Calif.) 52 p CSCL 03B G3/90

N87-16729

Unclas 43221

TABLE OF CONTENTS

I. INTRODUCTION

This report describes the research results obtained in the period from May 15, 1986 to January 14, 1987 supported by NASA under Grant No. NAGW-319. In this period, the photoabsorption and fluorescence cross sections of HCl and H_2CO measured previously were published in a scientific journal. The photoabsorption and fluorescence cross sections of H_2O, D_2O, H_2S, D_2S, and CO in the 50-200 nm region were measured in this period. These quantitative data are currently needed for the determination of the formation and destruction rates of molecules in the interstellar medium. The accomplishment in this research period is summarized below.

II. RESEARCH ACCOMPLISHED

A. Photoabsorption and Photodissociation of HCl and H_2CO

The photoabsorption and fluorescence cross sections of the interstellar molecule, HCl, were measured in the 106-185 nm region. Sharp absorption bands appear at wavelengths shorter than 135 nm, however, the fluorescence cross sections for the absorption bands are generally very small, indicating that the excited states of HCl are strongly predissociative. Therefore, the photodissociation section is essentially equal to the photoabsorption cross section. The photodissociation rate of HCl by the interstellar radiation field can thus be calculated from the photoabsorption cross section measured. The results for the HCl measurement is summarized in a paper entitled "Quantitative

photoabsorption and fluorescence study of HCl in vacuum ultraviolet." This paper is attached as Appendix A, which has been published in the Journal of Chemical Physics.

The photoabsorption and fluorescence cross sections of the interstellar molecule, H_2CO, were measured in the 105-180 nm region. The VUV fluorescence produced from photoexcitation of H_2CO was dispersed and identified to be the CO(A-X) emission system. Fluorescence from the HCO photofragment was also observed at excitation wavelength shorter than 147.5 nm. No fluorescence from the H_2CO molecule was detected. The VUV excitation of H_2CO thus presumably leads to dissociation, namely, the photodissociation cross section is equal to the photoabsorption cross section. The photodissociation rate of H_2CO by the interstellar radiation field can thus be calculated from the photoabsorption cross section measured. The result for the H_2CO measurement is described in a paper entitled "Fluorescence from VUV excitation of formaldehyde." This paper has been published in the Journal of Chemical Physics which is attached as Appendix B.

B. Photoabsorption and Photodissociation of H_2O and D_2O

A windowless apparatus was constructed in this funding period and used to measure the photoabsorption and fluorescence cross sections of molecules in the extreme ultraviolet region. H_2O and D_2O were the molecules first chosen for this type of measurement. The oscillator strengths and the fluorescence quantum yields in the 50-190 nm region were determined from the

photoabsorption cross sections measured. The results were summarized in a paper entitled "Quantitative photoabsorption and fluorescence study of H_2O and D_2O at 50-190 nm." This paper has been published in Chemical Physics which is attached as Appendix C.

C. Photoabsorption and Photodissociation of H_2S and D_2S

The windowless apparatus was also used to measure the photoabsorption and fluorescence cross sections of H_2S and D_2S in the 49-240 nm region. Fluorescence from photoexcitation of H_2S appears at 49-97 nm, but not in the longer wavelength region. Fluorescence spectra were dispersed and used to identify the emitting species to be $H_2S^+(\tilde{A})$, $SH^+(A)$, and H(n>2). No emission from the H_2S molecule itself was detected, indicating that excitation of H_2S by VUV excitation leads to dissociation. Thus, the photodissociation rate of H_2S by the interstellar radiation field can be calculated from the photoabsorption cross section measured. The calculation of photodissociation rate will be reported in the next funding period.

The results for the measurements of H_2S and D_2S have been summarized in a paper entitled "Quantitative photoabsorption and fluorescence spectroscopy of H_2S and D_2S at 49-240 nm," which is attached as Appendix D. This paper has been accepted for publication in the Journal of Chemical Physics.

D. Photoabsorption Cross Section of CO

The photoabsorption cross section of CO was measured in the 88-101 nm region as shown in Fig. 1. A Ti thin film was used to

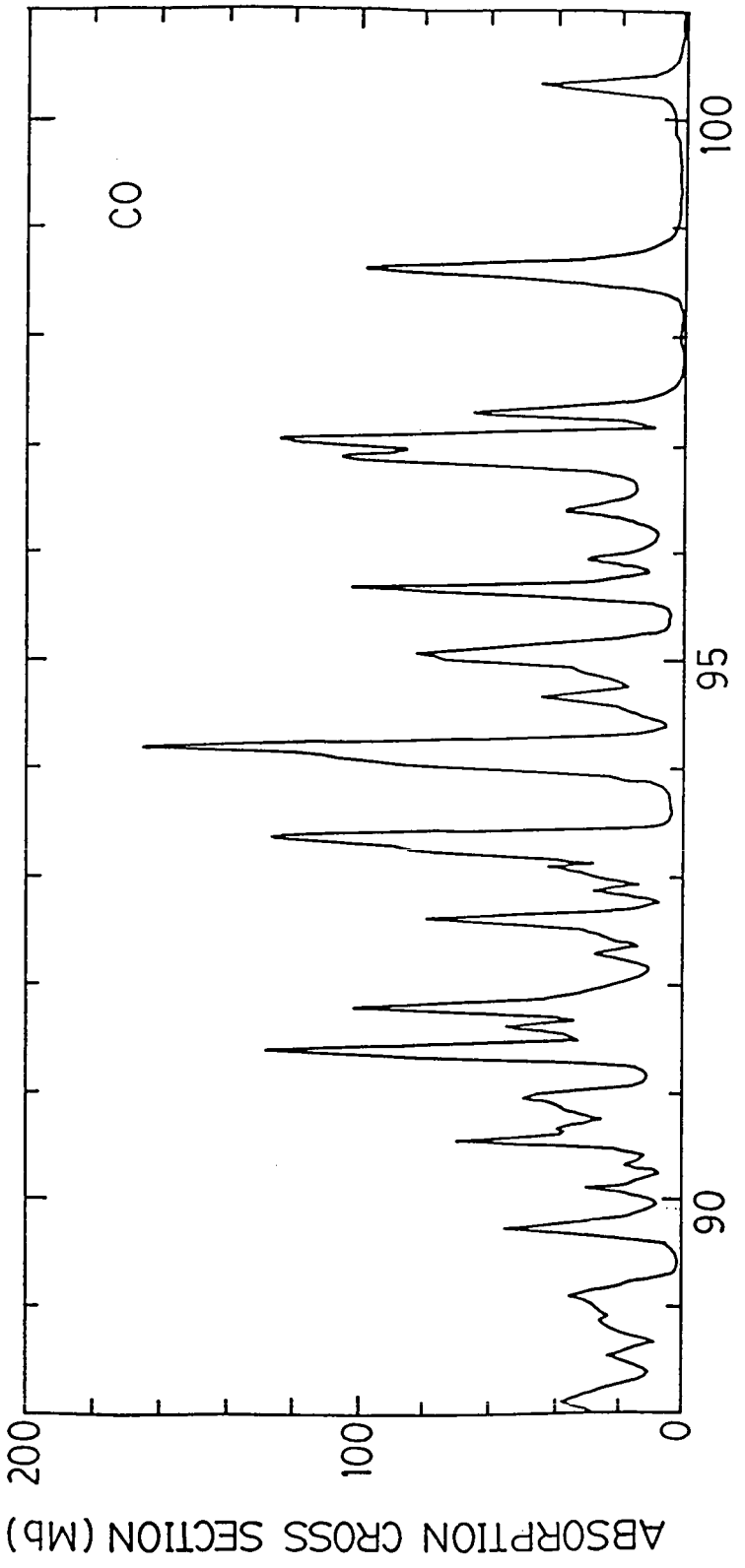

Fig. 1. Photoabsorption Cross Section of CO

cut-off the second-order light. Small photoabsorption cross section appears in the continuum region of 101-105 nm, however, the experimental uncertainty was very large. The photoabsorption cross section will be remeasured again in the next funding period. The photoabsorption cross section in the 91.2-110 nm region is currently needed for determining the photodissociation rate of CO in interstellar diffuse clouds as well as for calculating the penetration depth of VUV interstellar radiation into dense clouds.

III. Publications and Presentations in This Funding Period

1. L. C. Lee and M. Suto, "Photodissociation Processes of H_2O, D_2O, H_2S, and D_2S in VUV," presented at the XVII Informal Conference on Photochemistry, Boulder, Colorado, June 22-26, 1986.

2. M. Suto, X. Wang and L. C. Lee, "Photodissociation Processes of H_2CO and HCOOH in VUV," presented at the XVII Informal Conference on Photochemistry, Boulder, Colorado, June 22-26, 1986.

3. J. B. Nee and L. C. Lee, "Photodissociation of CS_2 at 193 nm," presented at the XVII Informal Conference on Photochemistry, Boulder, Colorado, June 22-26, 1986.

4. J. B. Nee, M. Suto and L. C. Lee, "Quantitative Photoabsorption and Fluorescence Study of HCl in Vacuum Ultraviolet" J. Chem. Phys., 85, 719 (1986).

5. M. Suto, X. Wang, and L. C. Lee, "Fluorescence from VUV Excitation of Formaldehyde", J. Chem. Phys., 85, 4228 (1986).

6. L. C. Lee and M. Suto, "Quantitative Photoabsorption and Fluorescence Study of H_2O and D_2O at 50-190 nm," Chem. Phys., 110, 161 (1986).

7. L. C. Lee, X. Wang, and M. Suto, "Quantitative Photoabsorption and Fluorescence Spectroscopy of H_2S and D_2S at 49-240 nm," J. Chem. Phys., in press (1987).

Quantitative Photoabsorption and Fluorescence Spectroscopy of H_2S and D_2S at 49-240 nm

L. C. Lee,[a] Xiuyan Wang, and Masako Suto
Department of Electrical & Computer Engineering
San Diego State University
San Diego, California 92182

ABSTRACT

Photoabsorption and fluorescence cross sections of H_2S and D_2S were measured in the 49-240 nm region using synchrotron radiation as a light source. Fluorescence from photoexcitation of H_2S appears at 49-97 nm but not in the longer wavelength region. Fluorescence spectra were dispersed, and used to identify the emitters to be $H_2S^+(\tilde{A})$, $SH^+(A)$ and H(n>2). The fluorescence quantum yield is about 6%. Photoexcitation of D_2S at 49-96 nm produces fluorescence with a quantum yield of about 5%. The emitters are identified from the fluorescence spectra to be $D_2S^+(\tilde{A})$, $SD^+(A)$, and D(n>2). The Franck-Condon factors for the SH^+ and SD^+ (A-X) transitions were determined. The SD(A-X) fluorescence was observed from photoexcitation of D_2S at 100-151 nm, for which the fluorescence cross section and quantum yield were measured.

a) Also, Department of Chemistry, San Diego State University

I. INTRODUCTION

The photoabsorption process of H_2S has been extensively investigated,[1-10] but little is known about the photodissociation process in the vacuum ultraviolet (VUV) region. The valence electronic orbitals of H_2S are similar to those of H_2O, so they would be expected to have similar photodissociation processes. Since VUV excitation of H_2O produces $OH(A^2\Sigma^+ - X^2\Pi)$ fluorescence,[11] it would be expected that photoexcitation of H_2S would produce $SH(A^2\Sigma^+ \rightarrow X^2\Pi)$ fluorescence. However, the SH(A-X) fluorescence was not detected.[12] This negative result has been explained by the observation[13-15] that SH(A) is highly predissociative, because the lifetime of SH(A) is very short (<5 ns). On the other hand, the lifetime of SD(A) is about 190 ns;[13,14] thus, SD(A) is not highly predissociative, and VUV photoexcitation of D_2S may produce SD(A-X) fluorescence. The observation of such fluorescence is reported in this paper.

Fluorescence from the $H_2S^+(\tilde{A}^2A_1-\tilde{X}^2B_1)$ system has been observed by a controlled-low-energy electron excitation of H_2S and the fluorescence spectrum has been analyzed.[16,17] Recently, Ibuki[18] dispersed the fluorescence spectra produced from photoexcitation of H_2S by the NeI (73.6 nm) and HeI (58.4 nm) resonance lines. For the NeI excitation, fluorescence is mainly from the excited $H_2S^+(\tilde{A})$ ion, and for the HeI excitation, additional fluorescence from the excited H(n>2) atoms is observed. The fluorescence spectra produced at other VUV lines are investigated in this experiment. In addition to the $H_2S^+(\tilde{A})$

and H(n>2) fluorescence, we also detected $SH^+(A-X)$ fluorescence from dissociative photoionization of H_2S, which was not detected by Ibuki.[18]

Similar to H_2S, fluorescences from the excited D_2S^+, SD^+ and D(n>2) species were observed from photoexcitation of D_2S. The absolute fluorescence cross section and quantum yield for both H_2S and D_2S were measured. The Franck-Condon factors for both the $SH^+(A-X)$ and $SD^+(A-X)$ systems were determined from the fluorescence spectra.

In addition to being of fundamental interest, the quantitative spectroscopic data of hydrogen sulfide are useful for the study of photochemistry occurring in the interstellar medium and the earth's upper atmosphere. Since H_2S is abundant in the interstellar medium,[19,20] the cross sections for various photoexcitation processes are needed to determine the destruction rate of H_2S by the interstellar radiation field. A significant amount of H_2S can be released from volcanoes and biogenic sources into the earth's atmosphere and the solar photodissociation rate of H_2S is needed for the atmospheric modeling.[21,22]

II. EXPERIMENT

A. Synchrotron Radiation Experiment

Synchrotron radiation produced from the electron storage ring of the University of Wisconsin was used to measure the photoabsorption and fluorescence cross sections. The experimental setup has been described in previous papers.[11,23]

In brief, synchrotron radiation was dispersed by a 1-m Seya vacuum monochromator with a grating blazed at 120 nm. The gas cell was 63.5 cm long with a 3.5 cm ID. Fluorescence was monitored by a photomultiplier tube (PMT, EMI 9558QB) sensitive in the 185-800 nm region in a direction perpendicular to the light beam. For wavelengths longer than 105 nm, a LiF window was used to separate the gas cell from the high vacuum monochromator. For wavelengths shorter than 105 nm, a porous window that had a 50% transmission for all wavelengths was used. Intensity of the second-order light was measured from the absorption and fluorescence spectra of N_2 under the same experimental conditions. The effect of the second-order light was corrected in the data analysis. The correct procedure has been described in a previous paper.[23] Measurements were performed at room temperature, 22°C. Light source intensity, electron beam current, gas pressure, and fluorescence intensity were simultaneously monitored and analyzed by an IBM-XT microcomputer.

H_2S was supplied by Matheson with a purity better than 99.5%. D_2S was supplied by Merck with a D-atom of 99.2%. The gases were used as delivered. Gas pressure was monitored by an MKS Baratron manometer.

B. Dispersing Fluorescence Experiment

The experimental setup for dispersing the fluorescence was essentially the same as that described in the earlier papers.[23,24] In brief, a capillary-condensed discharge light source was used to produce intense atomic emission lines in the

40-150 nm region. Each emission line was isolated by a 1-m vacuum monochromator (McPherson 225) with a grating blazed at 80 nm. The discharge light source was differentially pumped and separated from the high vacuum monochromator by a porous window with a transmittance of 50%. The light source entered a gas cell of 5 inch length and 3 inch ID through a narrow slit (no window between the gas cell and the vacuum monochromator). Fluorescence was dispersed by an 0.3-m monochromator (McPherson 218) and detected by a PMT (EMI 9558QB). The signal was processed by an ORTEC counting system.

III. RESULTS AND DISCUSSION

A. H_2S

1. Photoabsorption Cross Section and Oscillator Strength

The photoabsorption cross section of H_2S is shown in Figs. 1-3. The data were taken with monochromator resolutions of 0.2, 0.04 and 0.3 nm for the wavelength regions of 49-106, 106-160, and 160-240 nm, respectively. The uncertainty was estimated to be within 10% of the given value. Data in the 55-103 nm region agree very well with the results reported by Ibuki et al.[10] In the 120-160 nm region, the absorption spectrum shows sharp structures as observed in the earlier spectra.[1,2,7] The absorption cross section for a sharp band depends on the monochromator resolution. The current cross sections for the absorption structures are different from the data of Watanabe and

Jura,[1] although they agree very well for the absorption continuum at 160-210 nm.

The current absorption cross section was measured at low gas pressures so that the saturation of absorption at a rotational line was avoided and the measured cross section could be used to calculate the oscillator strength that did not depend on monochromator bandwidth. The method for calculating oscillator strength from the measured absorption cross section has been described in an earlier paper.[25] Oscillator strengths and integrations of absorption cross sections for various wavelength regions are listed in Table I. The measured oscillator strengths are useful for comparison with theoretical calculations.[9,26,27] The oscillator strength for the absorption continuum at 161-240 nm measured in this experiment is 0.0542. This value is comparable with the calculated values of 0.075[9] and 0.06.[26]

The absorption bands in the 120-240 nm region have been assigned[4,6,8,28,29] to the Rydberg states converging to the first ion state $\tilde{X}(2b_1^{-1})$ at 118.46 nm.[7,8] The Rydberg assignment given by Masuko et al.[7] is indicated in Fig. 2. The intense atomic-like ($2b_1 \rightarrow nd$) Rydberg series was observed by Baig et al.[8] up to n=26. They attributed the anomalously weak intensity for the n=9 and 10 members to interchannel interactions between this Rydberg series and some Rydberg states converging to the second ion state, $\tilde{A}(5a_1^{-1})$. The weak structures shown in the 90-120 nm region have been assigned[10,30] to the vibrational levels of Rydberg series converging to the $\tilde{A}$ ion state.

The $5a_1 \rightarrow 4s$ Rydberg transition has been calculated by Shih et al.[26] to be a relatively broad band around 132.0 nm with an oscillator strength of 0.11. This Rydberg transition was also calculated by Rauk and Collins[9] to be around 130.0 nm with an oscillator strength of 0.1729. Using the ionization potential of the $5a_1$ orbital, Robin[4] estimated the vertical energy of the $5a_1 \rightarrow 4s$ transition to be 72000 cm^{-1} (139 nm). In summary, the Rydberg transition is expected to be in the 125-145 nm region. The oscillator strength for the absorption continuum in this wavelength region (see Fig. 2) is about 0.18, which is close to the theoretical calculations.[9,26] These results suggest that the $5a_1 \rightarrow 4s$ transition is indeed in the 125-145 nm region.

2. Fluorescence Cross Section and Quantum Yield

Fluorescence was observed from photoexcitation of H_2S at wavelengths shorter than 97.0 nm. The absolute fluorescence cross section was determined by comparing fluorescence intensity with the $N_2^+(B-X)$ fluorescence produced from photoexcitation of N_2 at wavelengths shorter than 66 nm for which the fluorescence cross section is known.[31] The PMT response was corrected using the fluorescence spectrum dispersed in this experiment. The fluorescence was essentially produced from the $H_2S^+(\tilde{A})$, $SH^+(A)$ and $H(n>2)$ excited species as discussed in the next section. The fluorescence cross section is shown in Fig. 1b. The experimental uncertainty was estimated to be within 30% of the given value. Fluorescence starts to appear at 97.0 nm. The cross section increases to about 3 Mb (1 Mb = 10^{-18} cm^2) at 93.0 nm and then

decreases with decreasing wavelength to about 1 Mb at 49.0 nm. The fluorescence cross section measured by Ibuki[18] at 73.6 nm is about 1 Mb, which is smaller than the current value by a factor of 2. The agreement is satisfactory, if both experimental uncertainties are considered.

The fluorescence quantum yield calculated from the ratio of fluorescence cross section to absorption cross section is shown in Fig. 4. The yield starts to appear at the (0,0,0) vibrational level of $H_2S^+(\tilde{A})$. The wavelengths for the vibrational levels given by Karlsson et al.[5] are shown in Fig. 4. The fluorescence yield is nearly constant of about 6% at wavelengths shorter than the v_2=5 level. The constant fluorescence yield indicates that contribution from the vibrational levels higher than v_2=5 is very small. Dixon et al.[16] have observed that many predicted branches at high v_2 values are absent from the optical emission spectrum, indicating that predissociation may occur. Their observation is supported by the current result.

The $H_2S^+(\tilde{A}, v_2>5)$ ions may predissociate into H_2+S^+ for which the threshold is at 92.7 nm.[16] Eland[33] has shown in the photoelectron-photoion coincidence experiment that the v_2=5 level does not predissociate, but the higher levels do. H_2S^+ may predissociate through the $1^4A''$ repulsive state.[34] The branching ratio for the production of $H_2S^+(\tilde{A})$ from photoionization of H_2S at 58.4 nm[35] is about 30%. This ratio is much larger than the fluorescence yield of about 6%, indicating that the emission efficiency for the $H_2S^+(\tilde{A})$ state is not high.

The $H_2S^+(\tilde{B}\ 1b_2^{-1})$ ion state does not emit strongly, because the fluorescence yield does not increase significantly at the threshold of 84.7 nm[5]. This result is consistent with previous experimental observations[30,32,33] and theoretical calculation[34] that $H_2S^+(\tilde{B})$ predissociates into SH^++H through the $1^4A'$ repulsive state.

For excitation wavelengths longer than 97 nm, the fluorescence intensity was too weak to be detected. This negative result was very surprising, because the OH(A-X) fluorescence was observed from photoexcitation of H_2O at 105-137 nm,[11] thus, the SH(A-X) fluorescence was expected to be observable if the lifetime of SH(A, v=0) is as long as 550 ns as measured by Becker and Haaks.[36] The non-fluorescence result is, in fact, consistent with recent measurements that the lifetime of SH(A, v=0) is about 0.5-2 ns given by Tiee et al.[13], (3±2) ns by Friedl et al.[14], and (3.2±0.3) ns by Ubachs et al.[15] SH(A) decays mainly through predissociation. Friedl et al.[14] estimated that the fluorescence efficiency of SH(A, v=0) is in the 10^{-3}-10^{-2} range. If the production yield of SH(A) from photoexcitation of H_2S in the VUV region is similar to that of OH(A) from H_2O[11] of about 10%, then the fluorescence yield will be in the 10^{-4}-10^{-3} range. This fluorescence yield is too small to be detectable in our experiment.

Tiee et al.[13] and Friedl et al.[14] also measured the fluorescence lifetime of SD(A) to be about 190 ns. This lifetime is sufficiently long that the predissociation rate of SD(A) is

not high and the SD(A-X) fluorescence may have an observable intensity. This expectation motivated us to study the photoexcitation process of D_2S. Since D_2S is isoelectronic with H_2S, a comparison between their photoexcitation processes is also of interest.

3. $H_2S^+(\tilde{A}-\tilde{X})$ and H Balmer Fluorescence

The fluorescence produced by photoexcitation of H_2S was dispersed to identify the emitting species. The fluorescence spectra produced at the excitation wavelengths of 70.0, 84.4, and 92.3 nm are shown in Figs. 5(a), 5(b), and 5(c), respectively, where the monochromator resolution was 2 nm. Wavelength positions for the three sub-bands of the $H_2S^+(\tilde{A}^2A_1 - \tilde{X}^2B_1)$ system[16-18] are indicated in Fig. 5 to identify the fluorescence spectra. At 92.3 nm, the photon energy is just high enough to photoionize H_2S into the $H_2S^+(\tilde{A}, v_2=6)$ vibrational level,[16,17] which is the highest level shown in Fig. 5(c). For wavelengths shorter than 91.5 nm, it is energetically possible to produce the $v_2>7$ levels. However, only emission from $v_2<7$ levels appears at 70.0 and 84.4 nm as shown in Figs. 5(a) and 5(b), respectively. The lack of fluorescence indicates that the $v_2>7$ levels are predissociative.[16-18]

The H(n>2 → n=2) Balmer series is expected to be produced from the SH(X) + H(n>3) process at wavelengths shorter than 77.5 nm, for which the thresholds are listed in Table II. The H fluorescence produced at 70.0 nm is quite weak, but it is strong at 55.5 nm as shown in Fig. 6. At the shorter excitation

wavelengths, the H-Balmer series could be produced by the S+H(1)+H(n) process, for which the thresholds are also listed in Table II. The dissociation energies of $D_o(SH-H)=3.91$ eV[37] and $D_o(S-H)=3.55$ eV[38] as well as the excitation energies of H(n) given by Moore[39] were used for the threshold calculations.

4. $SH^+(A-X)$ Fluorescence

As shown in Fig. 6, $SH^+(A^3\Pi \rightarrow X^3\Sigma^-)$ fluorescence is also produced when H_2S is excited at 55.5 nm. This SH^+ fluorescence was not observed in the Ibuki's experiment[18] using the HeI (58.4 nm) line, although this line has a sufficient energy to produce the fluorescence. In our experiment, however, the $SH^+(A-X)$ emission does appear in the fluorescence spectrum when H_2S is excited at 58.6 nm. The negative result in Ibuki's experiment may have been due to low detection effiency in the UV region.

The rotational emission spectrum of the $SH^+(A, v'=0 \rightarrow X, v''=0,1)$ transition has been analyzed by Rostas et al.[40] The rotational emission from $SH^+(A, v'=1)$ is very weak[40] and it does not appear in Fig. 6. The decomposition of $SH^+(A, v'=1)$ into the S^+ ion has been observed in the laser excitation experiment.[41] These results indicate that $SH^+(A, v'=1)$ is predissociative. In contrast to the weak emission for $SH^+(A, v'=1)$, the $SD^+(A, v'=1)$ level has a substantial emission intensity as discussed in the next section.

The $SH^+(A-X)$ fluorescence intensity at 55.5 nm is about 10% of the total intensity, where the response of the detection system is corrected. Taking the total fluorescence cross section at

55.5 nm to be 1.6 Mb as shown in Fig. 1, the fluorescence cross section for $SH^+(A-X)$ is about 0.16 Mb. The fluorescence spectrum can be used to determine the Franck-Condon factor.[24] If the transition moment is assumed to be constant, then the Franck-Condon factors for the $SH^+(A, v'=0 \rightarrow X, v''=0$ and 1) transitions are determined to be 1 : 0.39.

B. D_2S

1. Photoabsorption Cross Section and Oscillator Strength

The photoabsorption cross sections of D_2S in the wavelength regions of 49-105, 105-160, and 160-240 nm are shown in Figs. 7,8, and 3b, for which the resolutions are 0.2, 0.04 and 0.1 nm, respectively. The experimental uncertainty is estimated to be within 10% of the given value. The absorption spectrum of D_2S is very similar to that of H_2S, except for some differences discussed below.

The vibrational and rotational spacings of D_2S are generally smaller than those of H_2S, because the D atom is heavier than H. In the 120-160 nm region, the absorption structures of D_2S are sharper than those of H_2S, which may be due to the rotational spacing of D_2S being smaller than that of H_2S. This phenomenon of concentrated rotational lines is obviously illustrated in the 140 nm band of D_2S that does not show the rotational structure, but the corresponding band of H_2S at 139 nm shows three rotational branches. The rotational structure observed in the absorption spectrum of H_2S is generally not observed in D_2S.

The absorption bands of D_2S in the 120-160 nm region are Rydberg transitions, similar to those of H_2S. The oscillator strength and the integration of absorption cross section over wavelength were calculated from the measured absorption cross section, and the results are listed in Table III. Very little data exist for comparison.

Vibrational structure is observed in the absorption spectrum of H_2S at 180-210 nm (Fig. 3a). The vibrational structure becomes more prominent in the absorption spectrum of D_2S (Fig. 3b). The average vibrational frequency is about 1187 cm^{-1} for H_2S and 853 cm^{-1} for D_2S. These frequencies are slightly higher than the values[3] of 1118 and 822 cm^{-1} respectively, as given by Thompson et al.[3] They attributed these frequencies to the ν_2 vibrational mode. The absorption continuum[9,26] in this wavelength region consists of a Rydberg transition ($2b_1 \rightarrow 4s$) and a valence transition ($2b_1 \rightarrow \sigma^*$). It is likely that the vibrational structures are caused by the Rydberg states, because the vibrational frequencies are very close to the ν_2 frequencies[17] of the $\tilde{X}(^2B_1)$ ion state, which are 1164.65 and 841.4 cm^{-1} for H_2S^+ and D_2S^+, respectively. The core electronic configuration of a Rydberg state is usually similar to that of the converging ion state, so the vibrational frequencies of both the Rydberg and ion states are expected to be similar. The observed vibrational frequencies are also close to the values[17] of the ground state, $\tilde{X}(^1A_1)$, which are 1188.40 and 859 cm^{-1} for H_2S and D_2S, respectively. Recently, Engel et al.[42] calculated

the absorption cross section of H_2O in the 150-185 nm region and found that the vibrational structure superimposed on the absorption continuum is inherent with the potential surface of the $H_2O(\tilde{A}\ ^1B_1)$ state. Similar case may occur in H_2S, for which the theoretical calculation is of interest.[43]

2. $D_2S^+(\tilde{A}-\tilde{X})$ and D Balmer Fluorescence

As shown in Fig. 7b, fluorescence from photoexcitation of D_2S appears at wavelengths shorter than 96.2 nm. The fluorescence cross section has a maximum value of 3.5 Mb at 92.0 nm and then decreases to about 0.9 Mb at 49 nm. The fluorescence spectra produced from photoexcitation at 70.0, 84.4, and 92.3 nm are shown in Fig. 9. Similar to H_2S, the fluorescence is identified to be the $D_2S^+(\tilde{A}-\tilde{X})$ system, for which the wavelength positions of the $(0,v_2',0 - 0,v_2'',0)$ vibrational transitions assigned by Dixon et al.[16] are indicated in Fig. 9. At 92.3 nm, the highest vibrational level that emits is $v_2'=8$ as shown in Fig. 9. By subtracting the excitation energy (2.95 eV) of the $\tilde{A}(0,8,0)-\tilde{X}(0,0,0)$ transition[16,17] from the excitation photon energy of 92.3 nm (13.43 eV), the potential energy for the $D_2S^+(\tilde{X})$ ion state is 10.48 eV. This value is slightly higher than the ionization potential energy of 10.2 $\pm$ 0.2 eV measured by Dibeler and Rosenstock.[44] By subtracting the vibrational energy of 0.64 eV[16,17] from the excitation photon energy, the potential energy of $D_2S^+(\tilde{A})$ is determined to be 12.79 eV. The highest emitting vibrational level is $v_2=10$. Similar to $H_2S^+(\tilde{A})$, the

vibrational levels higher than this level are likely predissociative.

The fluorescence quantum yield in the 49-100 nm region is shown in Fig. 10. The threshold at 96.2 nm corresponds to the (0,0,0) ground vibrational level of $D_2S^+(\tilde{A})$. The potential energies of the $(0,v_2,0)$ vibrational levels given by Duxbury et al.[17] are indicated in Fig. 10. The fluorescence yield at wavelengths shorter than the v_2=9 level is essentially a constant of about 5%, indicating that contribution from the higher vibrational levels is small. The high vibrational levels of $D_2S^+(\tilde{A})$ predissociate into D_2+S^+ at a threshold of 13.43 eV[35], for which the wavelength position is indicated in Fig. 10. The $D_2S^+(\tilde{B})$ state may have a small fluorescence yield, because the yield does not increase at its threshold of 85 nm.[35]

Similar to H_2S, excitation of D_2S in the 49-75 nm region produces significant D(n>2 → n=2) Balmer series emission. The fluorescence spectra produced at 55.5 and 70.0 nm are shown in Fig. 11. The Balmer series produced at 70.0 nm are much smaller than that at 55.5nm, indicating that they are most likely produced from the S+D(1)+D(n) process, for which the threshold energies are listed in Table II. The thresholds were calculated from the dissociation energies of D_0(SD-D) = 4.40 eV (obtained from this experiment as discussed in the next section) and D_0(S-D) = 3.60 eV[38], as well as the excitation energies of D(n) given by Moore.[39]

3. $SD^+(A-X)$ Fluorescence

The $SD^+(A^3\Pi - X^3\Sigma^-)$ fluorescence from photoexcitation of D_2S at 55.5 nm is shown in Fig. 11. The $SD^+(A-X)$ system has been analyzed by Rostas et al.[40] In addition to emission from the $v'=0$ level, the $v'=1$ level also emits as shown in Fig. 11, indicating that the $v'=1$ level of $SD^+(A)$ does not predissociate as severely as that of $SH^+(A)$. Fluorescence intensity for the $SD^+(A-X)$ system is about 19% of the total fluorescence intensity, where the response of the detection system is corrected. The total fluorescence cross section at 55.5 nm is about 1.6 Mb (see Fig. 7), implying that the cross section for the $SD^+(A-X)$ system is about 0.3 Mb. If the transition dipole moment is assumed to be a constant, then the Franck-Condon factors for the $v'=0 \rightarrow v''=0$, 1, and 2 transitions of the $SD^+(A-X)$ system determined from the fluorescence spectrum are 1 : 0.71 : 0.20, respectively.

4. SD(A-X) Fluorescence

Since the fluorescence lifetime[13,14] of SD(A) is quite long, the SD(A-X) fluorescence is expected to be observable. The origins for the (0,0) and (1,0) vibrational transitions of SD(A-X) are 325.0 and 309.8 nm, respectively.[45,46] As expected, fluorescence appears in the 116-154 nm region as shown in Fig. 12, where both absorption and fluorescence cross sections were measured at a resolution of 0.1 nm. The absolute fluorescence cross section was obtained by comparing the SD(A-X) fluorescence intensity with the OH(A-X) intensity produced from photoexcitation of H_2O, for which the fluorescence cross section

is known.[11] The uncertainty for the fluorescence cross section is estimated to be within 30% of the given value.

The fluorescence cross section near the threshold is very small, where the excitation function is enlarged as shown in the upper right-hand corner of Fig. 12. The threshold wavelength is at 151.0 $\pm$ 0.1 nm. This threshold can be used to determine the dissociation energy at room temperature to be 4.40 $\pm$ 0.01 eV, where the excitation energy of SD(A) of 3.81 eV[38,45] is used in the calculation. This dissociation energy which is smaller than the value of 4.63 eV determined from the thermochemical data.[47]

As shown in Fig. 12, the fluorescence cross section shows a structure closely correlated with the absorption structure; and the fluorescence yield at an absorption peak is higher than that at the underneath absorption continuum, as shown in Fig. 13. These results indicate that SD(A) is mainly produced from a predissociation process, which involves an interaction between a Rydberg state and a repulsive state that dissociates into SD(A). For a comparison, OH(A) is produced through an optically-allowed state, $H_2O(\tilde{B}^1A_1)$.[48]

The maximum fluorescence yield for SD(A-X) is about 0.8% as shown in Fig. 13. Considering the fluorescence efficiency[14] of the SD(A) state to be 0.3 $\pm$ 0.1, the SD(A) production yield from photodissociation of D_2S is about 4%. The SD(A) fluorescence drops sharply at 118.5 nm which corresponds to the first ionization threshold. Similar cases have been observed[49] in H_2O

and D_2O for which the fluorescence yields drop at ionization thresholds.

As shown in Fig. 13, the fluorescence yield shows structure. This is quite different from the cases of H_2O and D_2O, for which the fluorescence yields are relatively smooth.[49] The fluorescence quantum yield represents the interaction strength between a Rydberg state and a repulsive state that leads to the production of SD(A). The yield provides useful information for determining the repulsive state.

IV. CONCLUDING REMARKS

The photoabsorption and fluorescence cross sections of H_2S and D_2S were measured in the 49-240 nm region. In the 49-92 nm region, the fluorescence quantum yields for the $\tilde{A}$-$\tilde{X}$ system of H_2S^+ and D_2S^+ are about 6% and 5%, respectively. In contrast, the fluorescence intensities from the excited H_2O^+ and D_2O^+ ions are too weak to be observable in the same experiment. On the other hand, the fluorescence yields for the A-X system of OH and OD by photoexcitation of H_2O and D_2O at 106-137 nm are quite large,[11,47] when compared with those of SH and SD. No emission is observed from the SH(A) that decays mainly through predissociation.[13,14]

Recently, the Rydberg transitions of H_2S and D_2S have been extensively investigated by multiphoton ionization spectroscopy[50] and high resolution absorption spectroscopy.[51] For the 117-153 nm wavelength region, our absorption spectrum is very similar to

the high resolution absorption spectrum[51] obtained by photograph plates at low gas pressures. These new results and our quantitative data provide additional information for a better understanding of the photoexcitation process of the molecules.

ACKNOWLEDGEMENT

We wish to thank P. W. Langhoff at the Indiana University for a preprint about their theoretical study of H_2S, M. N. R. Ashfold at the University of Bristol (U.K.) for a preprint about their high resolution studies of the electronic spectra of H_2S and D_2S, and R. Schinke at the Max-Planck-Institut für Stromungsforschung (Germany) for useful comments. We also thank Dr. M. J. Mitchell, Dr. R. S. Ram, Dr. W. C. Wang and Dr. C. Ye in our laboratory for useful discussion and suggestions. The synchrotron radiation facility of the University of Wisconsin is supported by NSF under Grant No. DMR-44-21888. This material is based on the work supported by the NSF under Grant No. ATM-8412618 and by the NASA under Grant No NAGW-319.

REFERENCES

1. K. Watanabe and A. S. Jursa, J. Chem. Phys. 41, 1650 (1964).
2. L. B. Clark and W. T. Simpson, J. Chem. Phys. 43, 3666 (1965).
3. S. D. Thompson, D. G. Carroll, F. Watson, M. O'Donnell and S. P. McGlynn, J. Chem. Phys. 45, 1367 (1966).
4. M. B. Robin, Higher Excited States of Polyatomic Molecules Vol I. (Academic Press, N.Y. 1974).
5. L. Karlsson, L. Mattsson, R. Jadrny, T. Bergmark, and K. Siegbahn, Phys. Scrip. 13, 229 (1976).
6. R. Roberge and D. R. Salahub, J. Chem. Phys. 70, 1177 (1979).
7. H. Masuko, Y. Morioka, M. Nakamura, E. Ishiguro, and M. Sasanuma, Can. J. Phys. 57, 745 (1979).
8. M. A. Baig, J. Hormes, J. P. Connerade, and S. P. McGlynn, J. Phys. B: Atom. Molec. Phys. 14, L 725 (1981).
9. A. Rauk and S. Collins, J. Molec. Spectrosc. 105, 438 (1984).
10. T. Ibuki, H. Koizumi, T. Yoshimi, M. Morita, S. Arai, K. Hironaka, K. Shinsaka, Y. Hatano, Y. Yagishita and K. Ito, Chem. Phys. Lett. 119, 327 (1985).
11. L. C. Lee, J. Chem. Phys. 72, 4334 (1980).
12. L. C. Lee and J. A. Guest, unpublished results (1980).
13. J. J. Tiee, M. J. Ferris, and F. B. Wampler, J. Chem. Phys. 79, 130 (1983).
14. R. R. Friedl, Wm. H. Brune, and J. G. Anderson, J. Chem. Phys. 79, 4227 (1983).

15. W. Ubachs, J. J. TerMeulen and A. Dymanus, Chem. Phys. Lett. 101, 1 (1983).

16. R. N. Dixon, G. Duxbury, M. Horani, and J. Rostas, Mol. Phys. 22, 977 (1971).

17. G. Duxbury, M. Horani, and J. Rostas, Proc. R. Soc. London, A 331, 109 (1972).

18. T. Ibuki, J. Chem. Phys. 81, 2915 (1984).

19. W. D. Watson, Rev. Mod. Phys. 48, 513 (1976).

20. A. Dalgarno and J. H. Black, Rep. Prog. Phys. 39, 573 (1976).

21. W. Jaeschke, H. Claude, and J. Herrmann, J. Geophys. Res. 85, 5639 (1980).

22. N. D. Sze and M. K. W. Ko, Atmos. Environ. 14, 1223 (1980).

23. L. C. Lee, X. Wang, and M. Suto, J. Chem Phys., 85, 4228 (1986).

24. D. L. Judge and L. C. Lee, J. Chem. Phys. 57, 455 (1972).

25. L. C. Lee and J. A. Guest, J. Phys. B: Atom. Molec. Phys. 14, 3415 (1981).

26. S. K. Shih, S. D. Peyerimhoff, and R. J. Buenker, Chem. Phys. 17, 391 (1976).

27. G. H. F. Diercksen and P. W. Langhoff, Chem. Phys. in press; P. W. Langhoff, private comm. (1986).

28. W. C. Price, J. Chem. Phys. 4, 147 (1936).

29. W. C. Price, J. P. Teegan, and A. D. Walsh, Proc. R. Soc. London, A 201, 600 (1950).

30. H. F. Prest, W. B. Tzeng, J. M. Brom, Jr., and C. Y. Ng, Int. J. Mass Spectrom. Ion Phys. 50, 315 (1983).

31. L. C. Lee, J. Phys. B: Atom. Molec. Phys. 10, 3033 (1977).

32. V. H. Dibeler and S. K. Liston, J. Chem. Phys. 49, 482 (1968).

33. J. H. D. Eland, Int. J. Mass Spectrom. Ion. Phys. 31, 161 (1979).

34. G. Hirsch and P. J. Bruna, Int. J. Mass Spectrom Ion Phys. 36, 37 (1980).

35. C. E. Brion and D. S. C. Yee, J. Electron Spectrosc. 12, 77 (1977), C. E. Brion, J. P. D. Cook and K. H. Tan, Chem. Phys. Lett. 59, 241 (1978).

36. K. H. Becker and D. Haaks, J. Photochem. 1, 177 (1972/73).

37. D. R. Stull and H. Prophet, "JANAF Thermochemical Tables," 2nd Ed. Natl. Stand. Ref. Data Ser., Natl. Bur. Stand. 37 (1971).

38. K. P. Huber and G. Herzberg, Constants of Diatomic Molecules (Van Nostrand Reinhold, New York 1979).

39. C. E. Moore, Atomic Energy Levels, Vol. I, Natl. Stand. Ref. Data Ser. NSRDS-NBS 35 (1971).

40. J. Rostas, M. Horani, J. Brion, D. Daumont, and J. Malicet, Mol. Phys. 52, 1431 (1984).

41. C. P. Edwards, C. S. Maclean, and P. J. Sarre, Mol. Phys. 52, 1453 (1984).

42. V. Engel, R. Schinke, and V. Staemmler, Chem. Phys. Lett. 130, 413 (1986).

43. R. Schinke, Private Communication (1986).

44. V. H. Dibeler and H. M. Rosenstock, J. Chem. Phys. 39, 3106 (1963).

45. D. A. Ramsay, J. Chem. Phys. 20, 1920 (1952).

46. J. W. C. Johns and D. A. Ramsay, Can. J. Phys. 39, 210 (1961).

47. M. W. Chase, Jr., J. L. Curnutt, J. R. Downey, Jr., R. A. McDonald, A. N. Syverud, and E. A. Valenzuela, J. Phys. Chem. Ref. Data, 11, 695 (1982).

48. F. Flouquet and J. A. Horsley, J. Chem. Phys. 60, 3767 (1974).

49. L. C. Lee, and M. Suto, Chem. Phys., in press.

50. M. N. R. Ashfold, J. M. Bayley, R. N. Dixon, and J. D. Prince, Chem. Phys. 98, 289 (1985); M. N. R. Ashfold and R. N. Dixon, Chem. Phys. Lett. 93, 5 (1982).

51. C. A. Mayhew, J.-P. Connerade, M. A. Baig, M. N. R. Ashfold, J. M. Bayley, R. N. Dixon, and J. D. Prince, to be published (1986).

TABLE I

Integration of cross section over wavelength, $\int\sigma(\lambda)d\lambda$, and oscillator strength, f, of H_2S.

Wavelength (nm)	$\int\sigma\, d\lambda$ (Mb.nm)	f (10^{-3})
49.0-55.0	125	522
55.0-91.0	1667	3484
91.1-106.0	726	857
106.0-109.0	140	137
109.0-121.2	425	367
121.2-121.8	20.0	15.3
121.8-122.2	7.3	5.5
122.2-123.3	33.7	25.3
123.3-123.9	11.6	8.6
123.9-124.5	9.2	6.8
124.5-125.7	47.6	34.4
125.7-126.2	7.4	5.3
126.2-126.8	12.7	9.0
126.8-128.7	42.1	29.1
128.7-129.6	47.6	32.3
129.6-130.8	44.3	29.6
130.8-131.8	21.2	13.9
131.8-132.5	11.7	7.6
132.5-133.5	32.8	20.9
133.5-138.5	98.1	60.1
138.5-140.0	96.6	56.4
140.0-141.7	106.3	60.6

TABLE I (continued)

Wavelength (nm)	$\int \sigma \, d\lambda$ (Mb.nm)	f (10^{-3})
141.7-144.0	65.5	36.2
144.0-145.9	24.9	13.4
146.0-147.0	20.0	10.5
147.0-148.1	8.7	4.5
148.1-149.5	19.4	9.9
149.5-150.5	21.8	10.9
150.5-151.2	15.6	7.8
151.3-152.4	24.4	12.0
152.4-153.2	4.6	2.2
153.2-156.5	36.3	17.2
156.5-159.3	9.9	4.5
160.0-240.0	181	54.2

TABLE II

Threshold energies and wavelengths for various dissociation process of H_2S and D_2S.

Process	E (eV)	λ (nm)
SH(X) + H(1)	3.91	317.1
+ H(2)	14.11	87.9
+ H(3)	16.00	77.5
SH(A) + H(1)	7.71	160.8
H + S + H(1)	7.66	161.8
+ H(2)	17.86	69.4
+ H(3)	19.75	66.8
+ H(4)	20.41	60.7
+ H(5)	20.72	59.8
+ H(6)	20.88	59.4
SD(X) + D(1)	4.40	281.8
+ D(2)	14.60	84.9
+ D(3)	16.50	75.1
SD(A) + D(1)	8.21	151.0
D + S + D(1)	8.00	155.0
+ D(2)	18.20	68.1
+ D(3)	20.09	61.7
+ D(4)	20.75	59.8
+ D(5)	21.06	58.4
+ D(6)	21.22	58.5

TABLE III

Integration of cross section over wavelength, $\int \sigma(\lambda) d\lambda$, and oscillator strength, f, of D_2S.

Wavelength (nm)	$\int \sigma d\lambda$ (Mb.nm)	f (10^{-3})
49.0-55.0	111	461
55.0-91.0	1779	3729
91.1-106.0	768	905
106.0-108.0	94.6	93.4
108.0-119.0	407	361
119.0-121.0	48.9	38.4
121.0-121.4	12.0	9.3
121.5-122.1	20.2	15.4
122.2-122.6	6.9	5.2
122.6-123.5	29.6	22.1
123.6-124.1	8.9	6.6
124.2-126.6	68.4	49.2
126.6-127.5	20.3	14.3
127.5-128.4	23.1	15.9
128.4-129.0	14.9	10.2
129.0-129.8	47.1	31.8
129.9-130.7	39.5	26.3
130.7-133.2	54.4	35.2
133.2-133.8	22.5	14.3
133.8-138.8	106	64.3
138.8-139.9	107	62.2
139.9-141.7	108	61.2

TABLE III (continued)

Wavelength (nm)	$\int \sigma d\lambda$ (Mb.nm)	f (10^{-3})
141.7-144.5	72.2	39.9
144.6-146.7	23.6	12.6
146.7-148.4	23.1	12.0
148.4-149.4	15.8	8.0
149.5-150.4	11.4	5.7
150.4-152.5	49.9	24.7
152.5-159.9	39.3	18.4
160.0-240.0	189	54.5

FIGURE CAPTIONS

Fig. 1. (a) photoabsorption and (b) fluorescence cross sections of H_2S in the 49-110 nm region. The resolution is 0.2 nm. The cross sections are in units of Mb (10^{-18} cm^2).

Fig. 2. Photoabsorption cross section of H_2S in the 106-160 nm region. The resolution is 0.04 nm. The wavelength positions for the Rydberg states and the ion state given by Masuko et al. are indicated.

Fig. 3. The photoabsorption cross sections of (a) H_2S and (b) D_2S in the 160-240 nm region. The resolution is 0.3 nm for H_2S and 0.1 nm for D_2S. The average vibrational frequencies are 1187 cm^{-1} for H_2S and 853 cm^{-1} for D_2S.

Fig. 4 Fluorescence quantum yield for photoexcitation of H_2S in the 49-100 nm region. The wavelength positions for the v_2 vibrational levels of $H_2S^+(\tilde{A})$ given by Karlsson et al. are indicated. The thresholds for the production of $H_2S^+(\tilde{B})$ and H_2+S^+ are indicated.

Fig. 5. Fluorescence spectra produced from photoexcitation of H_2S at 70.0, 84.4, and 92.3 nm. The resolution is 2 nm. The wavelength positions for the $\tilde{A}(0,v_2',0)$-$\tilde{X}(0,v_2'',0)$ system of H_2S^+ given by Dixon et al. are indicated,

Fig. 6. Fluorescence spectra produced from photoexcitation of H_2S at 55.5 and 70.0 nm. The emission bands of SH^+(A-X) and H Balmer series are indicated.

Fig. 7. (a) absorption and (b) fluorescence cross sections of D_2S in the 49-110 nm region. The resolution is 0.2 nm.

Fig. 8. Absorption cross section of D_2S in the 105-160 nm region. The resolution is 0.04 nm.

Fig. 9. Fluorescence spectra produced from photoexcitation of D_2S at 70.0, 84.4, and 92.3 nm. The wavelength positions of the $D_2S^+(\tilde{A}-\tilde{X})$ system given by Dixon et al. are indicated.

Fig. 10. Fluorescence quantum yield for photoexcitation of D_2S in the 49-100 nm region. The wavelength positions for the v_2 vibrational levels of $D_2S^+(\tilde{A})$ given by Duxbury et al. and the threshold for the production of D_2+S^+ are indicated.

Fig. 11. Fluorescence spectra produced from photoexcitation of D_2S at 55.5 and 70.0 nm. The emission bands of $SD^+(A-X)$ and D Balmer series are indicated.

Fig. 12. (a) absorption and (b) fluorescence cross sections of D_2S in the 116-153 nm region. The fluorescence is the SD(A-X) band. The spectra in the 143-153 nm region are enlarged as shown in the upper right-hand corner. The resolution is 0.1 nm.

Fig. 13. The quantum yield of the SD(A-X) fluorescence produced from photodissociative excitation of D_2S in the 116-144 nm region. The line is drawn for eye-guide.

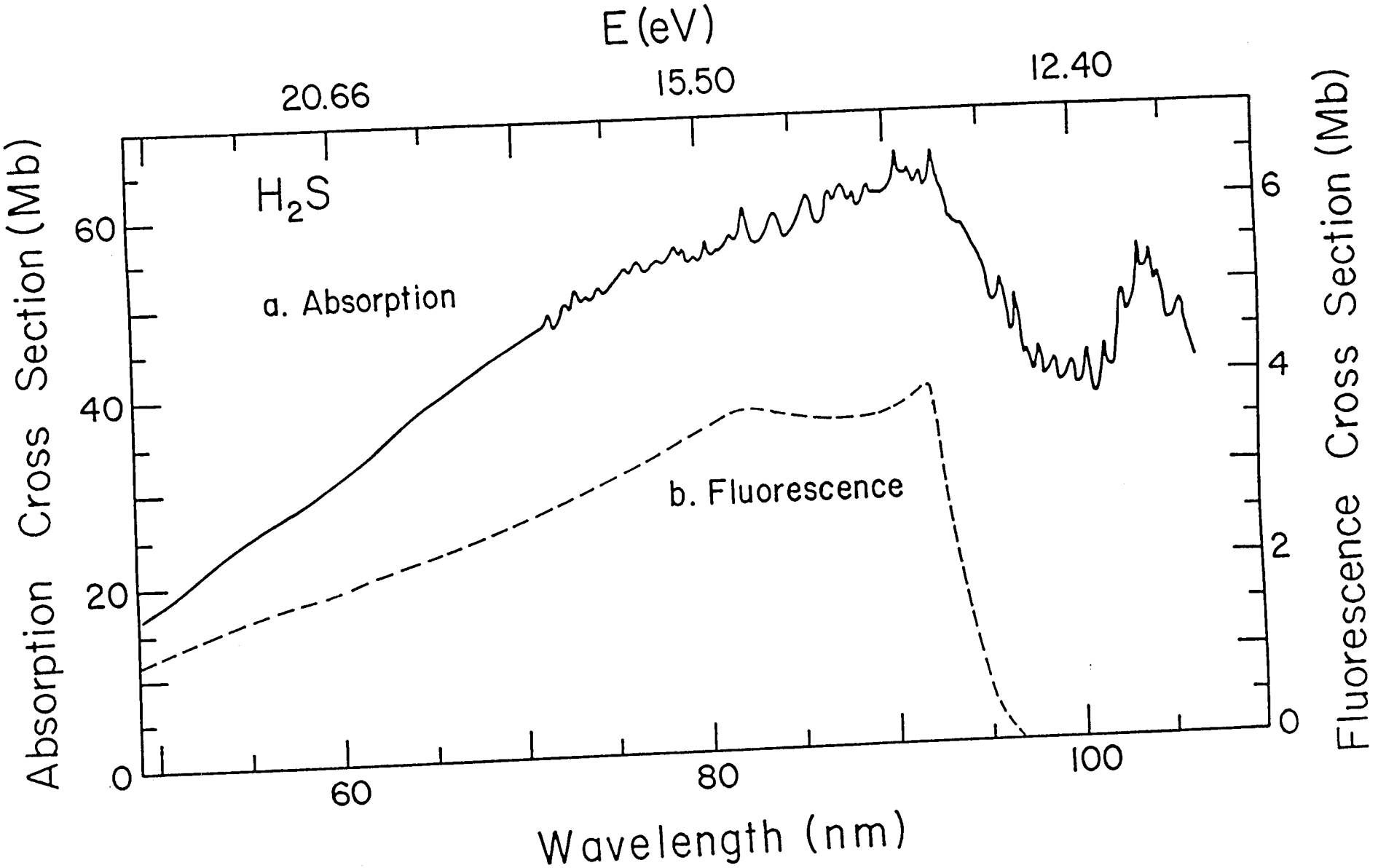
E (eV)
20.66
15.50
12.40
H_2S
a. Absorption
b. Fluorescence
Absorption Cross Section (Mb)
Fluorescence Cross Section (Mb)
0
20
40
60
0
2
4
6
60
80
100
Wavelength (nm)

Fig. 1

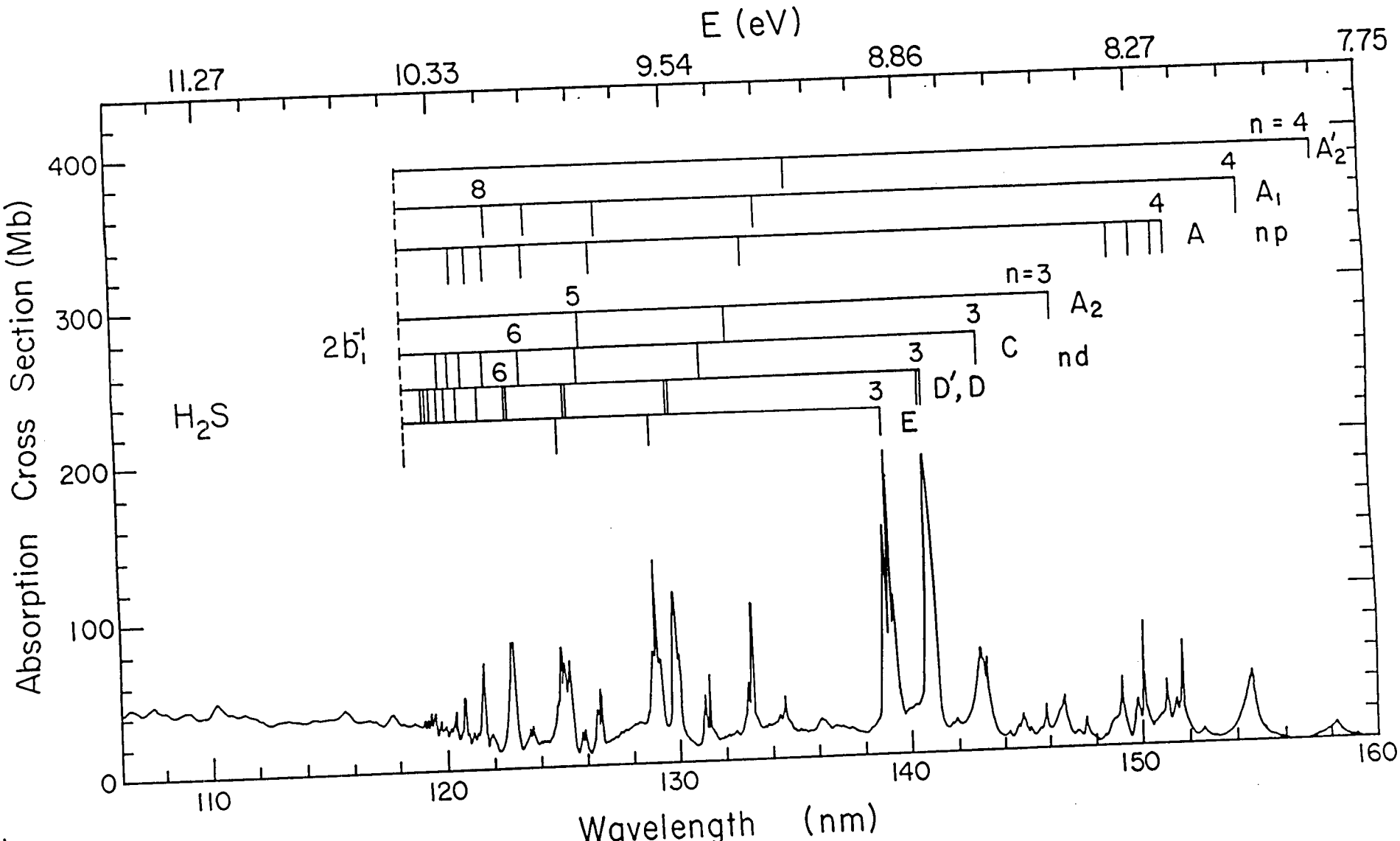
E (eV)
11.27
10.33
9.54
8.86
8.27
7.75
n = 4
A'2
4
A1
8
4
A
np
n=3
5
A2
3
6
C
nd
3
6
D', D
3
E
2b1-1
H2S
Absorption Cross Section (Mb)
400
300
200
100
0
110
120
130
140
150
160
Wavelength (nm)

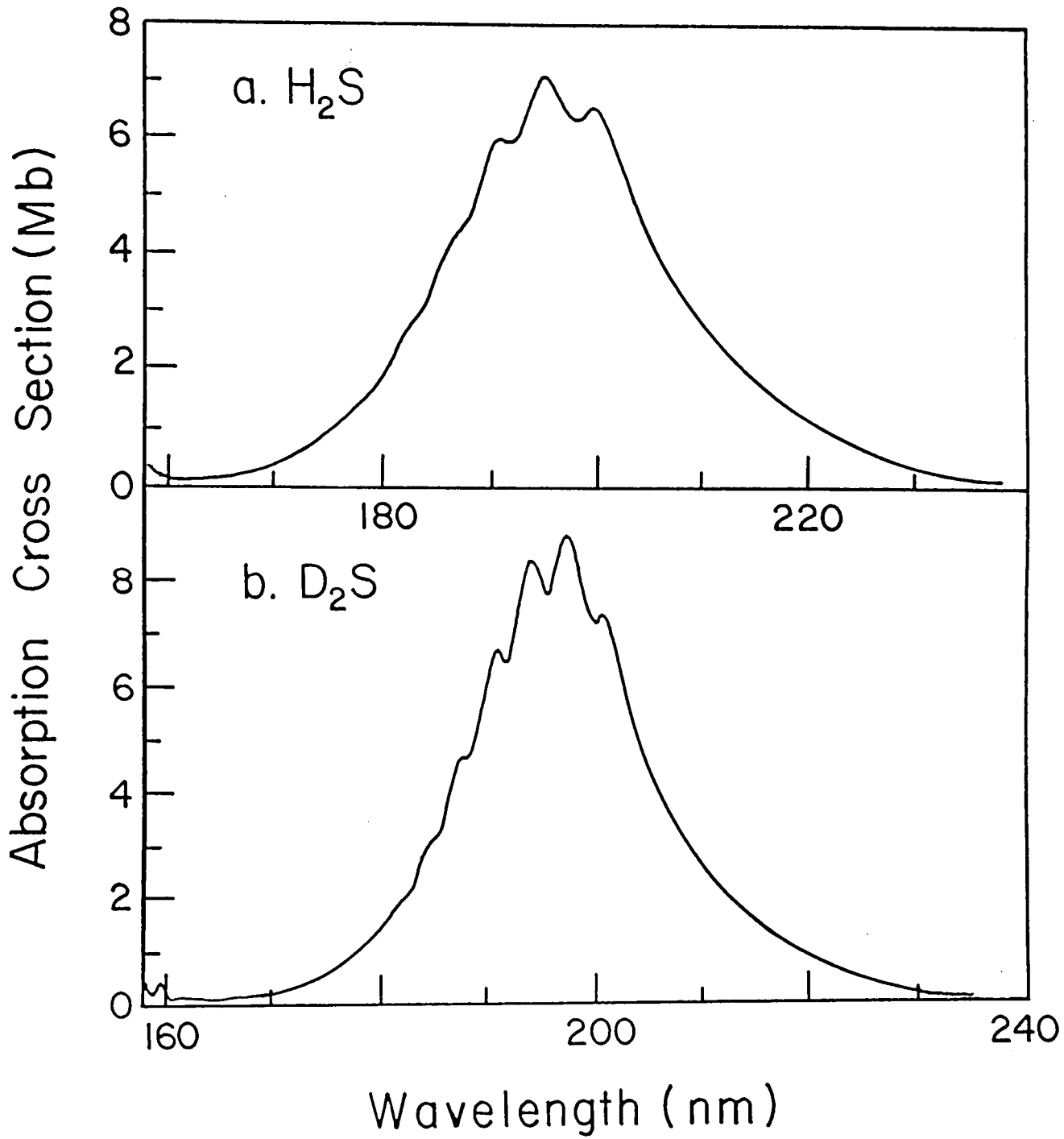
a. H_2S
b. D_2S
Absorption Cross Section (Mb)
Wavelength (nm)
0
2
4
6
8
160
180
200
220
240

Fig. 4

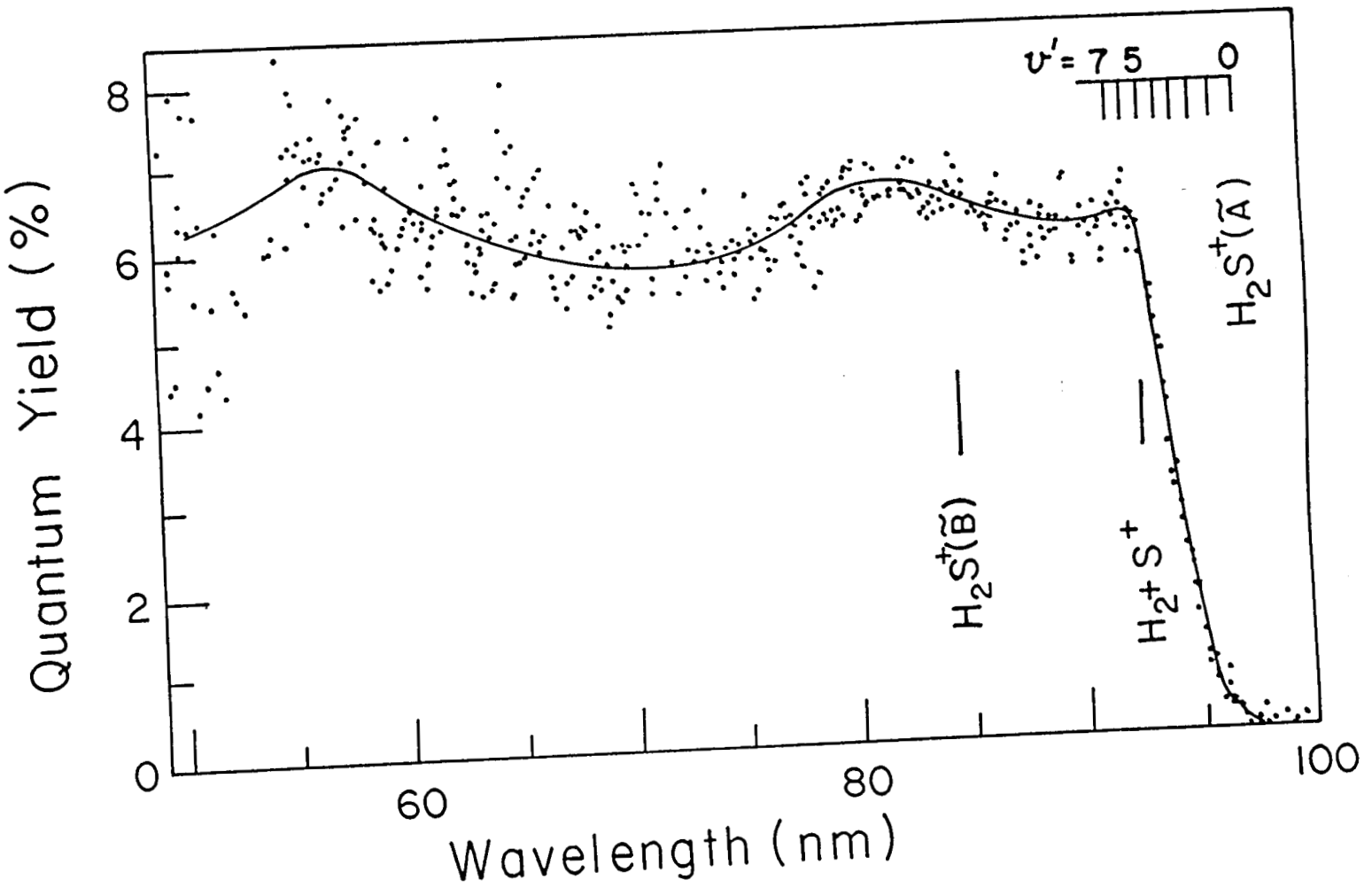
Quantum Yield (%)
0
2
4
6
8
60
80
100
Wavelength (nm)
v' = 7 5 0
H2S+(Ã)
H2S+(B̃)
H2+ S+

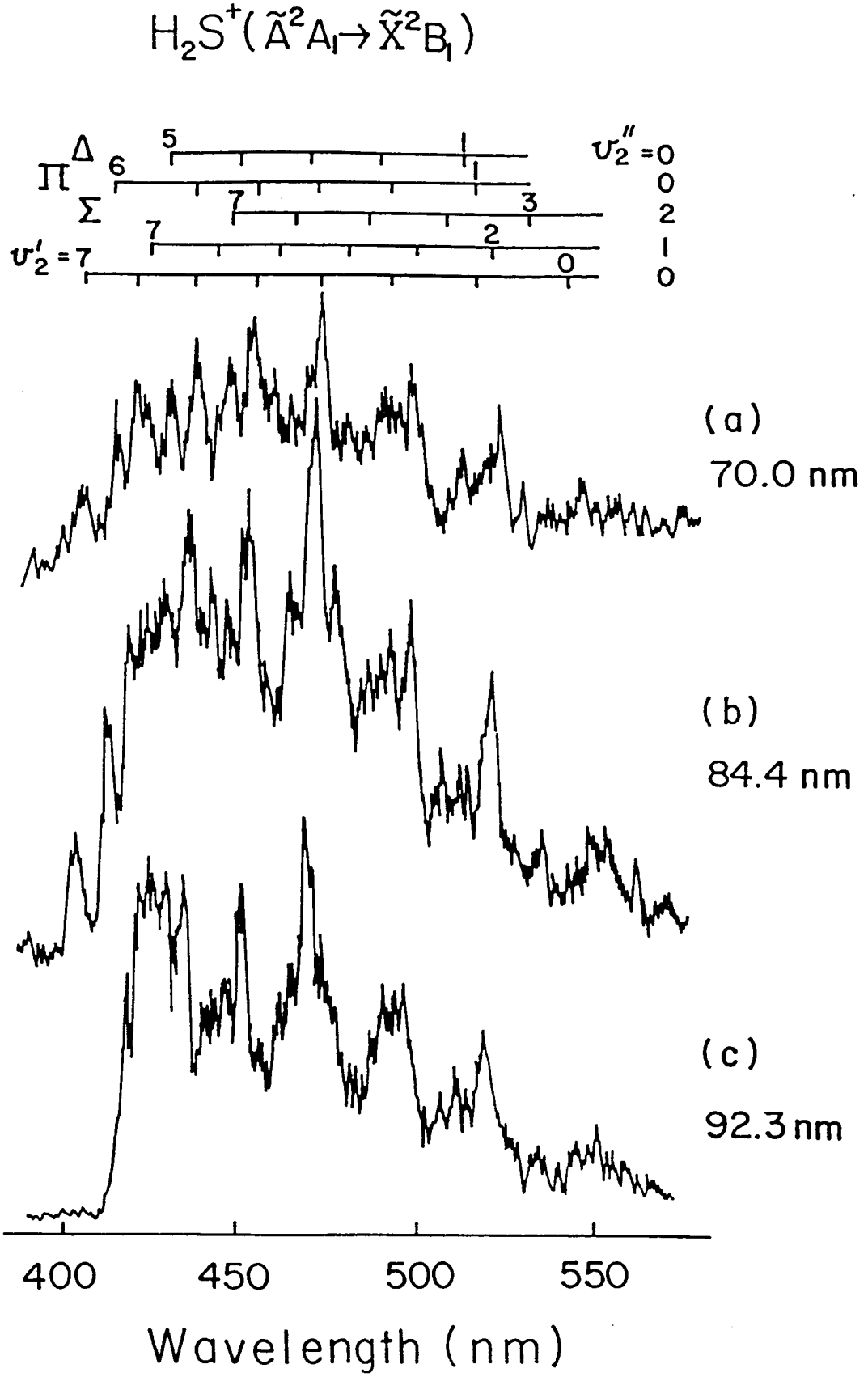
$H_2S^+(\tilde{A}^2A_1 \rightarrow \tilde{X}^2B_1)$
Π
Δ
Σ
$\upsilon_2' = 7$
5
6
7
7
1
3
2
0
$\upsilon_2'' = 0$
0
2
1
0
(a)
70.0 nm
(b)
84.4 nm
(c)
92.3 nm
400
450
500
550
Wavelength (nm)

Fig. 5

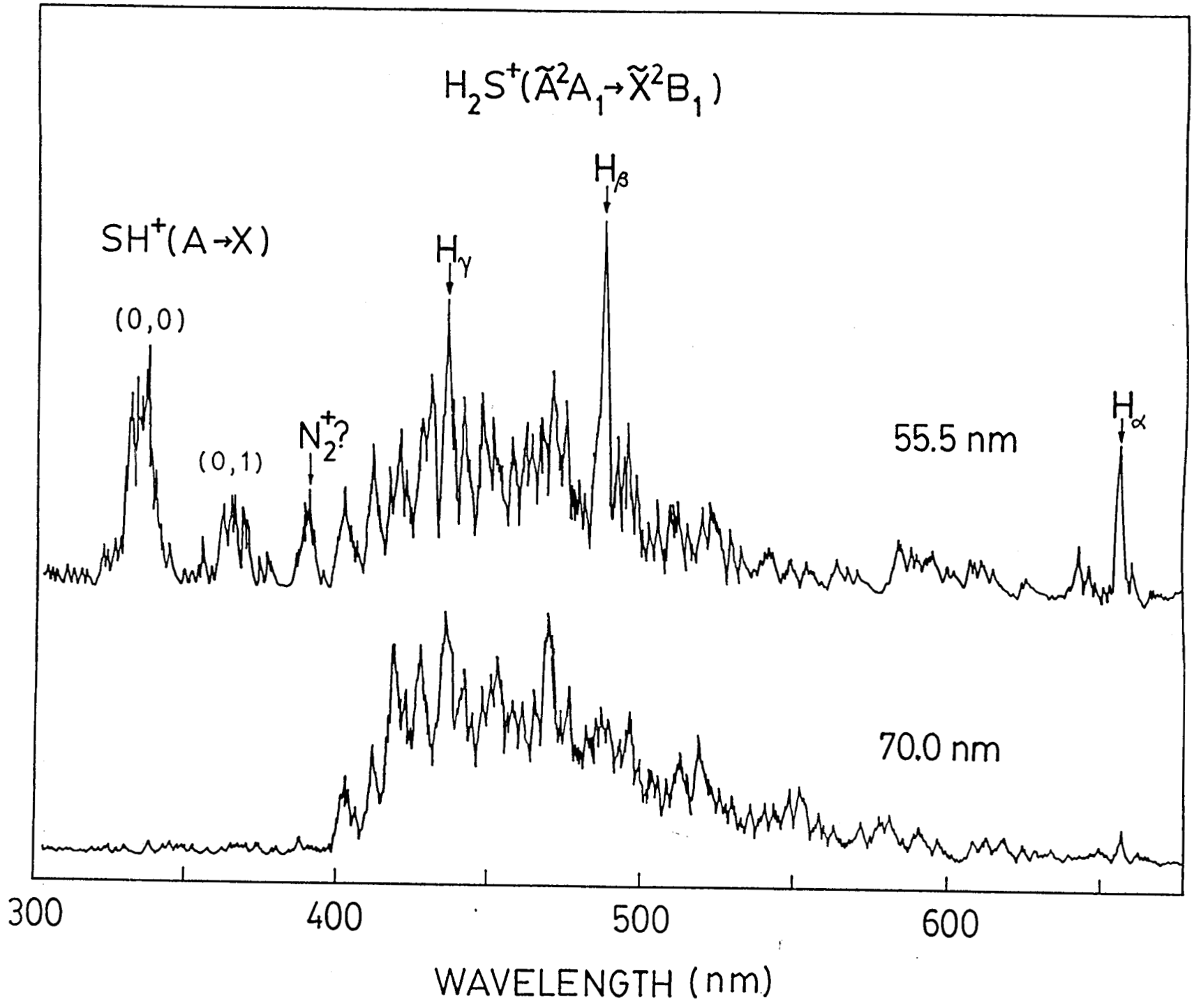
$H_2S^+(\tilde{A}^2A_1 \rightarrow \tilde{X}^2B_1)$
$SH^+(A \rightarrow X)$
(0,0)
(0,1)
N_2^+?
H_γ
H_β
H_α
55.5 nm
70.0 nm
300
400
500
600
WAVELENGTH (nm)

Fig. 2

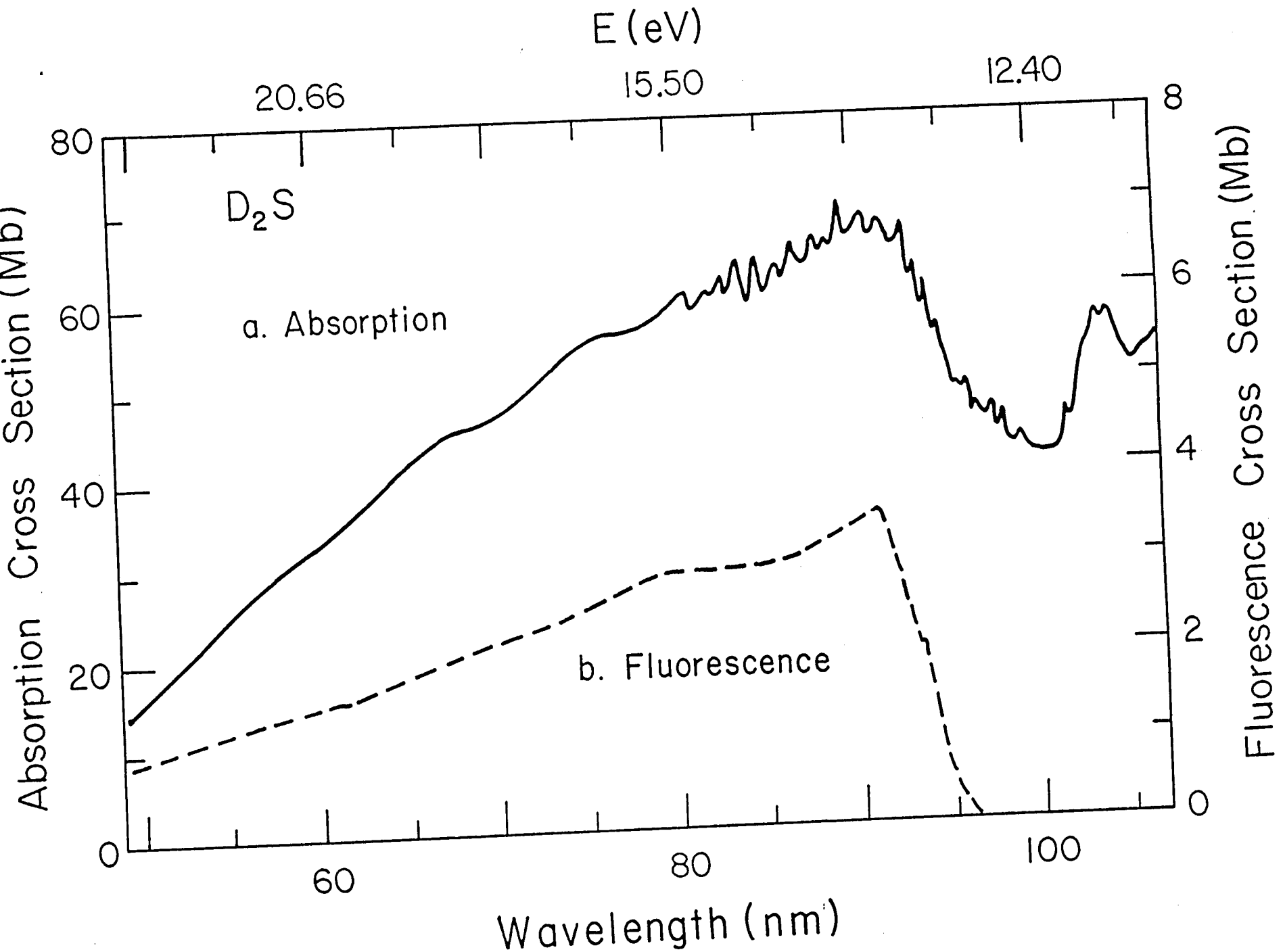
E (eV)
20.66
15.50
12.40
80
60
40
20
0
8
6
4
2
0
D_2S
a. Absorption
b. Fluorescence
Absorption Cross Section (Mb)
Fluorescence Cross Section (Mb)
60
80
100
Wavelength (nm)

Fig. 7

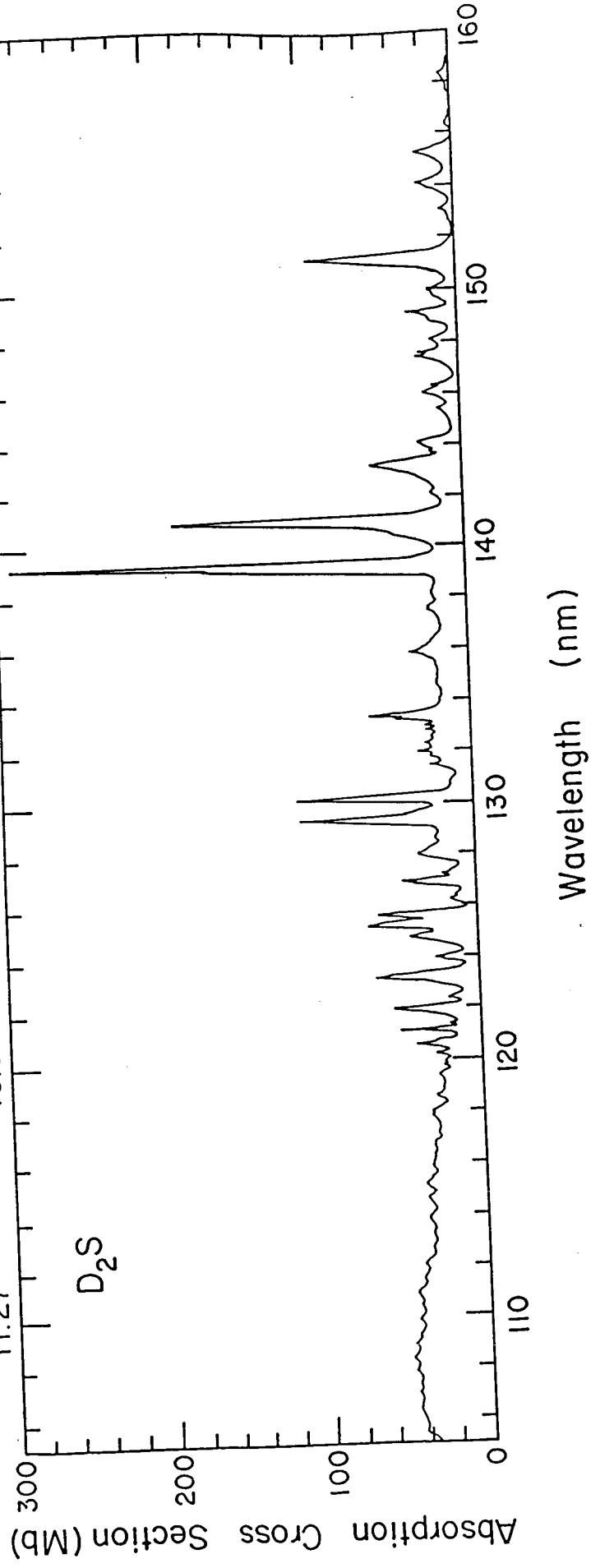
Absorption Cross Section (Mb)
300
200
100
0
E (eV)
11.27
10.33
9.54
8.86
8.27
7.75
Wavelength (nm)
110
120
130
140
150
160
D_2S

Fig. 8

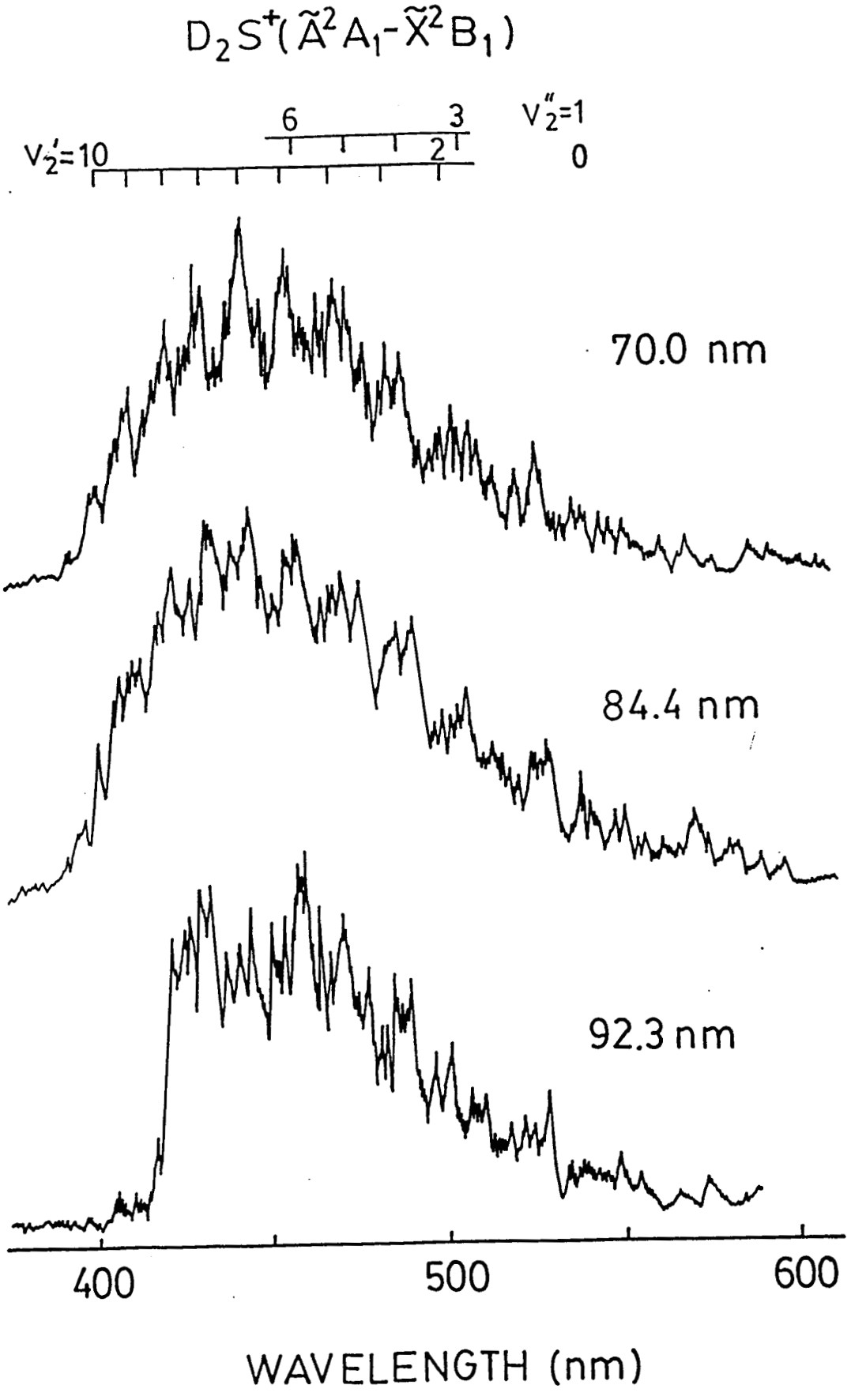
$D_2S^+(\tilde{A}^2A_1-\tilde{X}^2B_1)$
V_2'=10
6
3
2
V_2''=1
0
70.0 nm
84.4 nm
92.3 nm
400
500
600
WAVELENGTH (nm)

Fig. 9

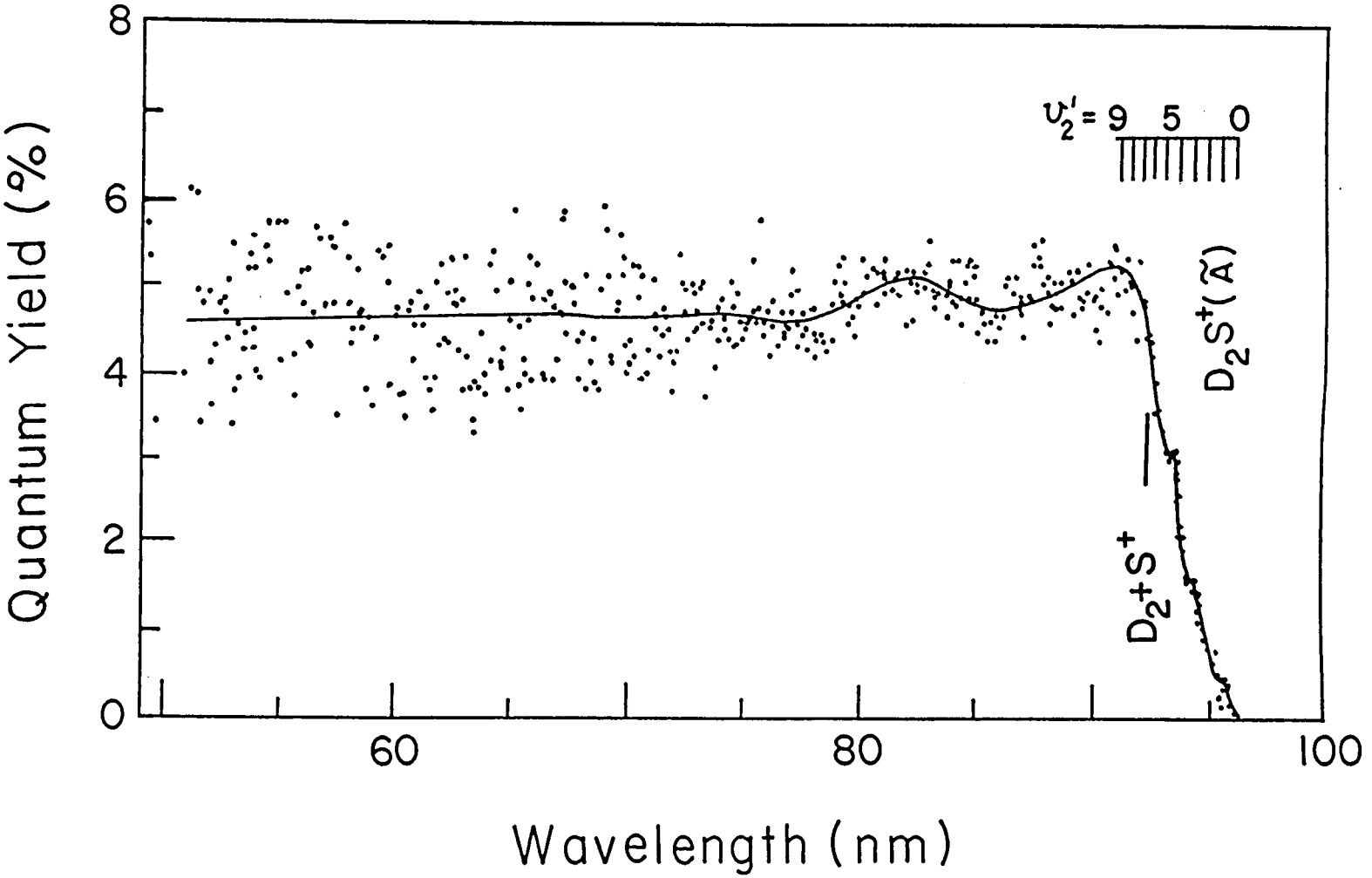
Quantum Yield (%)
0
2
4
6
8
60
80
100
Wavelength (nm)
v_2' = 9 5 0
$D_2S^+(\tilde{A})$
D_2+S^+

FIG. 10

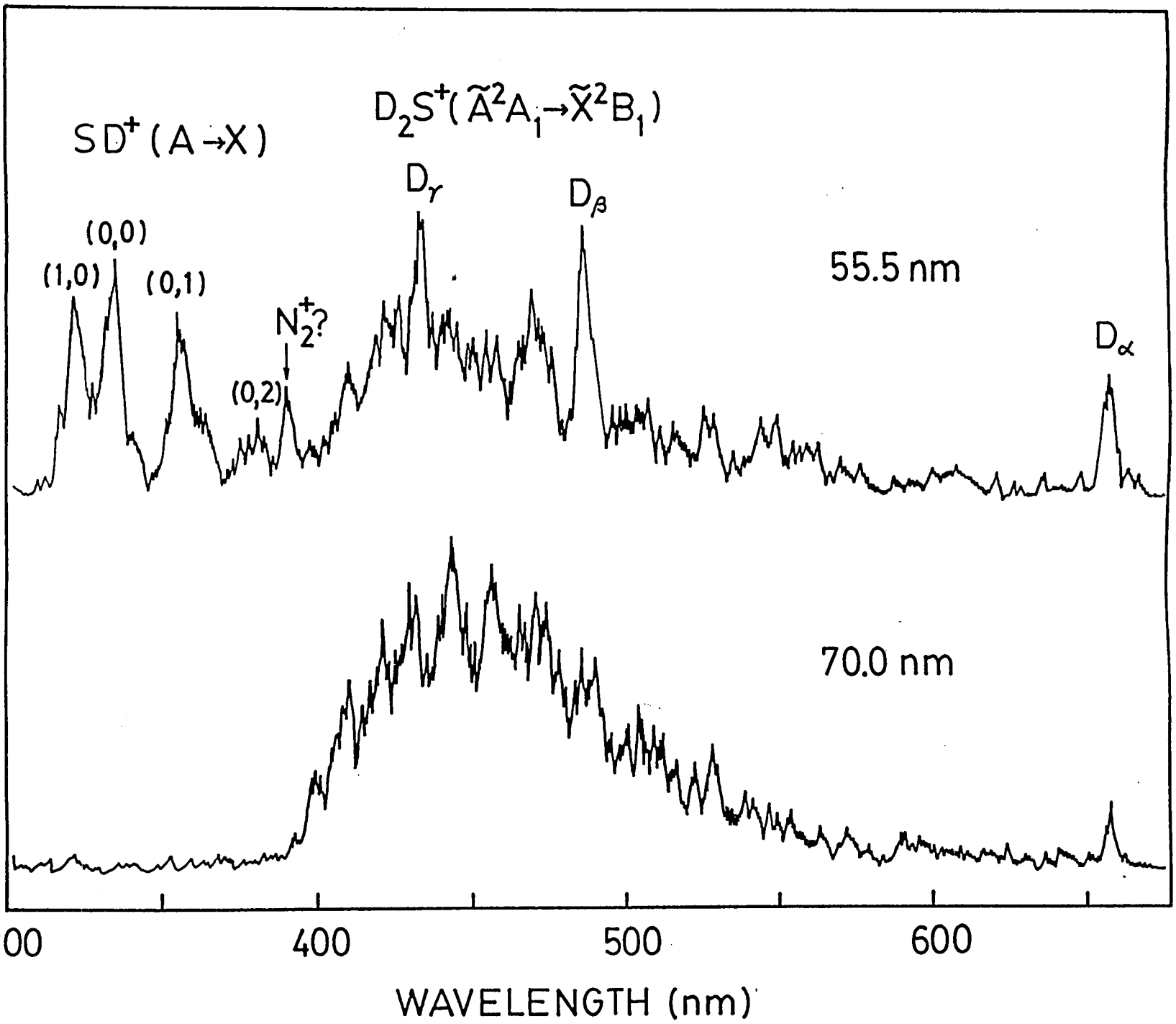
SD+ (A→X)
D2S+(Ã2A1→X̃2B1)
Dγ
Dβ
(0,0)
(1,0)
(0,1)
N2+?
(0,2)
55.5 nm
Dα
70.0 nm
300
400
500
600
WAVELENGTH (nm)

Fig. 11

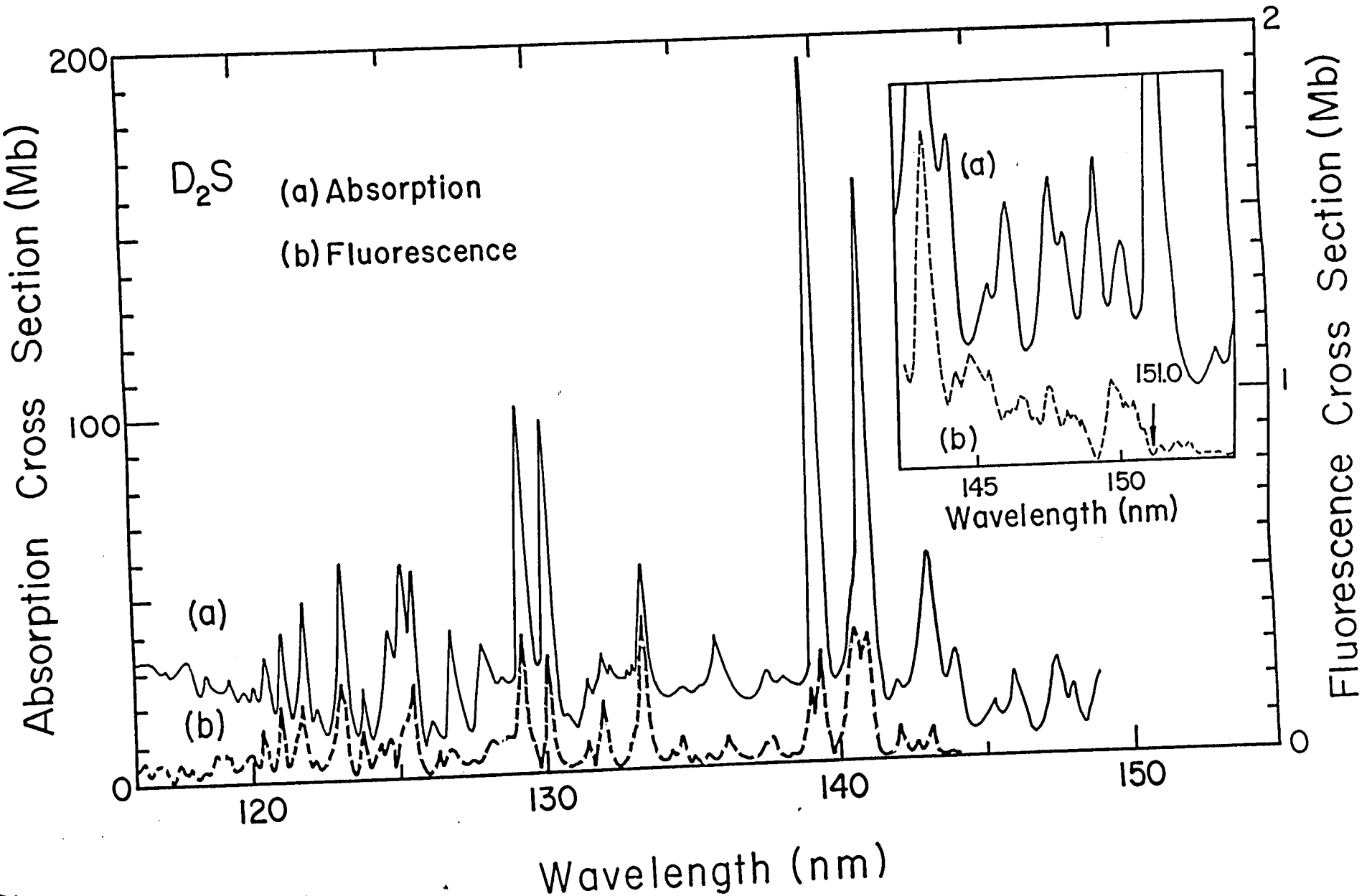
D2S
(a) Absorption
(b) Fluorescence
Absorption Cross Section (Mb)
Fluorescence Cross Section (Mb)
Wavelength (nm)
200
100
0
2
1
0
120
130
140
150
(a)
(b)
151.0
145
150
Wavelength (nm)

Fig. 12

Fig. 13